CALCULATION OF NANO-CRYSTALLINE COPPER TOUGHNESS USING THE EMBEDDED ATOM METHOD

A. Luque[1], J. Aldazabal[1], J.M. Martínez-Esnaola[1], J. Gil Sevillano[1]
[1]CEIT-Centro de Estudios e Investigaciones Técnicas de Gipuzkoa and
Escuela Superior de Ingenieros-Tecnun, University of Navarra
Paseo Manuel Lardizábal 15, 20018 San Sebastián, SPAIN

ABSTRACT

This work is an approach to the fracture simulation of nano-crystalline materials, using molecular dynamics techniques and the embedded-atom method (EAM). The studied microstructures were obtained through the Voronoi technique, with variable number of grains. Periodic-boundary conditions are also employed, in order to minimise the boundary effects. The simulations correspond to copper atoms. The mechanical behaviour of the microstructures has been analysed and compared with previous works. Special attention has been paid to fracture and mode-I toughness.

1 INTRODUCTION

The study of mechanical properties of nano-structured materials is becoming very popular in the last few years. As these materials are difficult to produce and manufacture, part of this research is made theoretically or using numerical simulations.

Nowadays, with the help of the powerful computers, it is possible to simulate the mechanical behaviour of these materials from an atomistic point of view. For these simulations, a small amount of atoms is considered. Knowing the position and the forces that appear among them, resulting from interatomic potentials, and applying the boundary conditions, it is possible to compute the trajectories of the atoms.

The biggest system simulated up to now following this method contains 10^9 atoms [1]. The present work analyses nano-metric two-dimensional copper samples containing 10000 atoms. These samples are loaded until fracture, thus giving the toughness values in mode-I.

2 SIMULATION METHOD

The simulation method used in the present work was the *embedded-atom method* (EAM) [2,3]. In this method each atom of the solid is treated as an "impurity" located in a crystal formed by the rest of atoms. From this point of view, the atom is subjected to two kinds of interactions: that caused by the surrounding atoms, and that originated by their electrons. The total energy of an atom is given by

$$E_i = \frac{1}{2}\sum_{j\neq i} V(r_{ij}) + F(r_{ti}) \tag{1}$$

The first term of this equation is known as *pair potential*. It represents the interaction between an atom and its surrounding neighbours. The second term is known as *embedding potential*, and corresponds to the interaction between the electronic orbitals of the atoms of the system. Finally, r_{ti} is a dimensionless parameter that represents the total electronic density in the atom position normalised by its value at equilibrium.

$$r_{ti} = \sum_{j\neq i} r(r_{ij}) \tag{2}$$

where $r(r_{ij})$ is related to the contribution of each atom to the electronic density.

Tabulated values corresponding to copper [4] were used to know the contribution of each atom, both in terms of the electronic density corresponding to the *embedding potential* and in terms of pair potential.

All the microstructures simulated in the present work are two-dimensional simulations. Thus it is necessary to modify the potentials defined for three-dimensional systems. The potentials were modified to get the same equilibrium distance between atoms in two and three-dimensional simulations [5]. The values of the *pair potential* (figure 1.a) are not modified as they only depend on the distance between atoms.

However, the *embedding potential* values not only depend on the interatomic distances but also on the number of surrounding neighbours, through the electronic density ρ. At equilibrium, the two-dimensional configuration has fewer neighbours than the three-dimensional case. To guarantee the same equilibrium distance for the 2D and the 3D cases, it is necessary to increase the electronic density of each atom, as shown in figure 1.b.

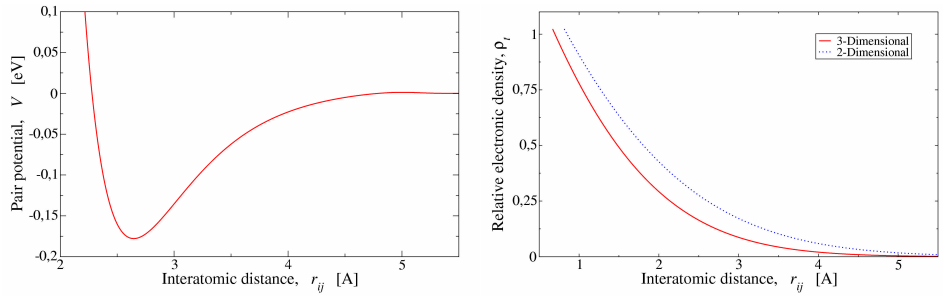

(a) (b)

Figure 1: (a) *Pair potential* of copper [4]. (b) Relative electronic density contributed by each neighbour as obtained for 3D simulations [4] and corrected for its use in 2D simulation [5].

Knowing the potentials that appear among atoms, the force acting over each atom can be computed. From these forces and the mass of the atoms it is possible to predict their trajectories, through the integration of the equations of motion [6]. This integration has to be solved using numerical methods with very small increments of time ($\Delta t \approx 1$ ps). Because of this, the Embedded Atom Method is restricted to simulate very short periods of time.

The present work assumes that the system temperature corresponds to 0 K. With this condition, the movement of atoms towards the equilibrium is quasi-static. To produce this movement all atoms are stopped, i.e. their velocities are set to zero, after each integration step.

3 GENERATION, RELAXATION ANDLOADING OF MICROSTRUCTURES

The five microstructures analysed in this paper were generated using Voronoi tessellation [7] with 1, 4, 8, 16 and 32 seeds. Once the seeds are randomly located in the simulated domain, the Voronoi cells are filled with close-packed copper atoms, forming grains. For each cell a random direction was used to define the orientation of the lattice. Periodical two-dimensional boundary conditions were used to minimise free surfaces effects [8].

The size of all the microstructures generated in this work is 250×250 $Å^2$. To guarantee the fracture of these virtual samples, an ellipsoidal notch, with dimensions $2a$=75 Å and $2b$=15 Å, was generated at the middle of the height. Because of the periodic boundary conditions, the elliptical cut corresponds to an infinite row of equally spaced notches.

Once the atoms are located in the microstructure and the notch is generated a relaxation process is applied. This process minimises the system energy by relaxing the stresses that locally appears in triple points and in grain boundaries [5]. Then, a tensile test of the virtual sample is simulated by fixing three boundaries of the system and moving the fourth one making the simulated domain bigger. The movement of the boundary in each step of the traction process is set to 10^{-4} Å.

Keeping in mind the concept of quasi-static test, once a tractive step is applied, the atoms move towards their equilibrium positions, relaxing the system. When the atoms get to the equilibrium, i.e. when the system energy between two consecutive relaxation steps does not decreases, the pressure on the system boundaries is calculated [9]. Knowing the displacement of the boundary and the system pressure the s-e plot is computed.

4 RESULTS

4.1 Mechanical Behaviour

Table 1 summarises the characteristics of the simulated microstructures. In this table, l_x is the width of samples, D, the average grain size and l_z the average distance between atoms at the system boundaries. In the simulations, the thickness of the simulated layer was assigned to be equal to l_z.

Table 1: General characteristics of simulated microstructures.

# grains	l_x [Å]	D [Å]	l_z [Å]	$E_{0.1\%}$ [GPa]
1	246.7	∞	2.3232	112
4	246.3	69.5	2.2536	118
8	245.7	49.0	2.2920	151
16	243.7	34.4	2.3065	114
32	241.8	24.1	2.3571	96

The mechanical behaviours predicted by the simulations performed in this work are similar to those obtained in previous works [10]. At the beginning of the simulation, all microstructures show a linear-elastic behaviour, with values of Young's modulus very close to the value 124 GPa, reported in the literature for pure copper [11]. The value obtained for each microstructure is listed in the right column of Table 1.

Following the linear region, a plastic behaviour begins. This behaviour corresponds to the generation, movement and interaction of dislocations inside the samples. Figure 2 was obtained changing the colour of atoms according to its energy [12]. Figure 2.a shows at the top of the microstructure two dislocations (light blue) generated during the plastic deformation of the sample. It is also possible to see in other simulations a small movement of the grain boundaries at this stage of the test.

Finally, in the fracture stage following the plastic region, it is possible to see intergranular fracture and cleavage. In all polycrystalline samples, both fracture mechanisms were observed at the same time. This phenomenon, illustrated in figure 2.b., has also been reported by other authors for nano-crystalline metals [13].

During cleavage, the crack grows along compact directions of the atomic lattice and, in the intergranular fracture, the crack grows by coalescence of nano-voids that appear in front of the crack tip.

Finally, the stress strain plots of the five simulated microstructures are shown in figure 3.

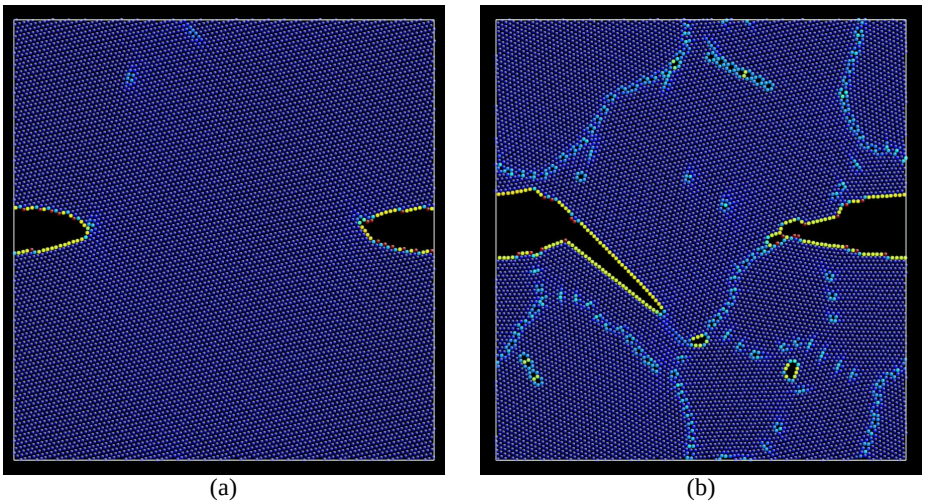

(a) (b)

Figure 2: (a) Emission and movement of dislocations in the single-crystalline sample and (b) combined fracture mode (cleavage on the left and intergranular on the right) on poly-crystalline sample. Colours of atoms change according to their energy, blue means low energy and red high energy values.

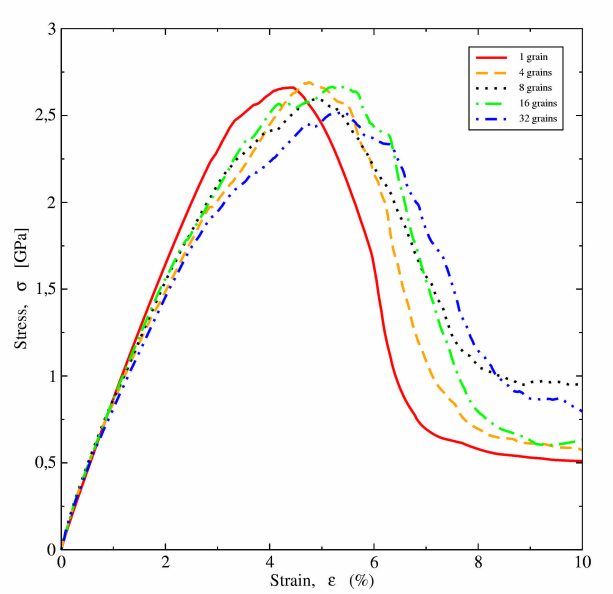

Figure 3: *s-e* plots obtained from the simulated microstructures. The elastic, plastic and fracture stages can be clearly distinguished.

4.2 Energy approach to the toughness

During the virtual tensile test, the simulated microstructure increases its energy. At the beginning, the energy is elastically stored (increasing the interatomic distance) and later in a non-reversible way (generating and moving dislocations). When fracture takes place, the crack grows catastrophically. An energetic criterion for determining the initiation of fracture in quasi-static conditions is given by [14]:

$$dW = dU + G_c dA \tag{3}$$

where W is the external work introduced into the system, U is its internal energy, G_c is the critical energy release rate and A is the crack size.
From eqn. (3) the following expression can be derived:

$$G_c = -\frac{d(U-W)}{dA} = -\frac{1}{l_z}\frac{dU}{da} \tag{4}$$

where l_z is the mean interatomic distance and a the crack length.
The material toughness in terms of the critical stress intensity factor, K_{Ic}, is then given by

$$K_{Ic} = \sqrt{\frac{G_c E}{1-n^2}} \tag{5}$$

where E is Young's modulus and n the Poisson's ratio of the material. The values E=124 GPa and n=0.343 [15] have been used in the calculations.
Table 2 shows in the second and third columns the toughness values obtained using this energetic criterion. The error bars are an estimate of the lack of precision measuring the crack length.

Table 2: Summary of toughness values obtained for copper using the two methods used in present work. The number in brackets indicates the equation used to get the values.

D [Å]	$G_c^{(4)}$ [J/m^2]	$K_{Ic}^{(5)}$ [kPam$^{1/2}$]	$K_{Ic}^{(6)}$ [kPam$^{1/2}$]
∞	1.97 ± 0.19	526 ± 26	457 ± 37
69.5	2.27 ± 0.33	564 ± 41	656 ± 81
49.0	2.72 ± 0.23	619 ± 26	404 ± 28
34.4	2.020 ± 0.060	534.0 ± 8.0	750 ± 110
24.1	4.29 ± 0.47	776 ± 42	622 ± 73

4.3 Stress approach to the toughness

Considering that the simulated system corresponds to a configuration of infinite cracks equally spaced in horizontal direction, the critical stress intensity factor can be written as [16]:

$$K_{Ic} = s_c \sqrt{pa_c} \sqrt{\frac{l_x}{pa_c}\tan\frac{pa_c}{l_x}} \tag{6}$$

where a_c is the critical crack size and s_c is the critical applied stress.
Table 2 shows in the fourth column the values of the critical stress intensity factor in mode-I obtained using this stress criterion. The error bars were obtained, as described in the previous subsection.

5 CONCLUSIONS

The results from these simulations, although obtained for two-dimensional microstructures, give realistic behaviours of copper from the atomistic point of view.

As in previous works, the simulations predict three different stages in the mechanical behaviour: elastic, plastic and fracture.

The last stage is characterised by the simultaneous occurrence of cleavage and intergranular fracture. The amount of each fracture mode varies with the grain size.

ACKNOWLEDGEMENTS

The work presented in this paper has been made under the sponsorship of the "Education, Universities and Research Council of the Basque Government" and the "Ministry of Science and Technology (MCyT)", Spain, under projects EX2002-6 and MAT2003-04314. A. Luque thanks to the "Fundación de Centros Tecnológicos – Iñaki Goenaga" for the PhD grant received.

REFERENCES

[1] Bulatov V., "Crystal plasticity from defect dynamics", NATO Advanced Study Institute, Fréjus, France, 2-13 September (2002).

[2] Daw M.S., Baskes M.I., "Semiempirical, quantum mechanical calculation of hydrogen embrittlement in metals", Phys. Rev. Lett., **50**, 1285-1288 (1983).

[3] Daw M.S., Baskes M.I., "Embedded-atom method: Derivation and application to impurities, surfaces, and other defects in metals", Phys. Rev. B, **29**, 6443-6453 (1984).

[4] Mishin Y., Farkas D., Mehl M.J., Papaconstantopoulos D.A., "Structural stability and lattice defects in copper: Ab initio, tight-binding, and embedded-atom calculations", Phys. Rev. B, **63**, 224106 (2001).

[5] Luque A., "Simulación atomística del comportamiento a fractura de materiales nanocristalinos", Licence Thesis, University of Navarra, San Sebastián, 22-23 (2003).

[6] Raabe D., "Computational Materials Science", Ed. Wiley-VCH, 101-102 (1998).

[7] Torquato S., "Random Heterogeneous Materials: Microstructure and Macroscopic Properties", Springer, 189-192 (2002).

[8] Allen M.P., Tildesley D.J., "Computer Simulation of Liquids", Oxford University Press, 24-32 (1987).

[9] Ercolessi F., "A molecular dynamics primer", Spring College in Computational Physics, ICTP, Trieste, 24-25 (1997).

[10] Luque A., Aldazabal J., Gil Sevillano J., "Simulación atomística del comportamiento a fractura de materiales nanocristalinos", Anales de Mecánica de la Fractura, **20**, 107-112 (2003).

[11] Ashby M.F., Jones D.H.R., "Engineering Materials 1: An Introduction to the Properties and Aplications", Ed. Butterworth-Heinemann, 31 (1995).

[12] Li J., "AtomEye: an efficient atomistic configuration viewer", Modelling Simul. Mater. Sci. Eng., **11**, 173-177 (2003).

[13] Van Swygenhoven H., Derlet P.M., Hasnaoui A., "Atomistic Modelling of Strength of Nanocrystalline Metals", Advanced Engineering Materials, **5**, 345-350 (2003).

[14] Ashby M.F., Jones D.H.R., "Engineering Materials 1: An introduction to the Properties and Applications", Ed. Butterworth-Heinemann, 121-122 (1995).

[15] "Material information: Copper", Goodfellow, http://www.goodfellow.com, (On line August 2003).

[16] Anderson T.L., "Fracture Mechanics: Fundamentals and Applications", Ed. CRC Press, 47-48 (1995).